Bioelectrochemistry 94 (2013) 69–74

Contents lists available at ScienceDirect

Bioelectrochemistry

journal homepage: www.elsevier.com/locate/bioelechem

Oxygen biosensor based on bilirubin oxidase immobilized on a nanostructured gold electrode

Marcos Pita [a,*], Cristina Gutierrez-Sanchez [a,1], Miguel D. Toscano [b], Sergey Shleev [c,2], Antonio L. De Lacey [a,*]

[a] Instituto de Catalisis y Petroleoquimica, Consejo Superior de Investigaciones Cientificas, C/Marie Curie 2, L10, 28049 Madrid, Spain
[b] Department of Protein Diversity, Novozymes A/S, Krogshøjvej 36, 2880 Bagsværd, Denmark
[c] Biomedical Sciences, Faculty of Health and Society, Malmo University, SE-205 06 Malmo, Sweden

ARTICLE INFO

Article history:
Received 11 June 2013
Received in revised form 26 July 2013
Accepted 27 July 2013
Available online 6 August 2013

Keywords:
Biocatalysis
Bilirubin oxidase
Biosensor
Direct electron transfer
Gold nanoparticles

ABSTRACT

Gold disk electrodes modified with gold nanoparticles have been used as a scaffold for the covalent immobilization of bilirubin oxidase. The nanostructured bioelectrodes were tested as mediator-less biosensors for oxygen in a buffer that mimics the content and the composition of human physiological fluids. Chronoamperometry measurements showed a detection limit towards oxygen of 6 ± 1 μM with a linear range of 6-300 μM, i.e. exceeding usual physiological ranges of oxygen in human tissues and fluids. The biosensor presented is the first ever-reported oxygen amperometric biosensor based on direct electron transfer of bilirubin oxidase.

1. Introduction

Bioelectrodes that use enzymes as catalysts are promising systems for both *in vivo* biosensing and implantable biofuel cells. Bioelectrodes can provide electric energy using the naturally existing biochemical substances as fuels and oxidants [1,2]. Electrochemical biosensors can take advantage of the specificity and selectivity of enzymatic processes to substitute the classic amperometric sensors, which are prone to false positive signals or poisoning under physiological conditions. An important advance would be developing an O_2 biosensor that could minimize the critical time to detect pathological O_2 imbalance and shorten the intervention time for first-aid professionals. Such biosensor may find practical applications both *in vitro* and *ex vivo* biomedical studies, as well as *in vivo* analysis. It is a widely held notion that low O_2 concentration yields to cell apoptosis, tissue damage and death. A biosensor that accomplishes such challenges has to cover a broad range of O_2 concentration. For instance, O_2 concentration in blood ranges 50–130 μM; [3] O_2 concentration in brain tissue and brain cerebrospinal fluid varies from 1 to 10 μM during a carotid compression up to approximately 100 μM on healthy conditions [4]. O_2 concentration in saliva ranges 2–10 μM [5]. Therefore, it is of great interest to develop an O_2 biosensor with a linear detection range from standard conditions in air-saturated water (0.26 mM) [6] to approximately 1 μM. An advance towards the application of implantable self-powered biosensors is to develop a bioelectrode that shares the same manufacturing technology with the powering biofuel cell cathode [9], avoiding the use of the scarce and expensive platinum as electrocatalyst. Another advantage of this biosensor would be the possibility of miniaturization, reaching electrodes far smaller than the commercial ones, sized in a diameter of 4 μm. On the other hand, classical O_2-detection electrodes [7,8] are interference-free thanks to a Teflon membrane, which can make the sensing process difficult.

Bilirubin oxidase (BOx) is a multicopper oxidase (MCO) that oxidizes several natural compounds while reducing O_2 directly to H_2O [10]. BOx performs its catalytic activity by means of four Cu ions split in two interconnected active sites, one to bind and oxidize the organic substrate and another one to bind and reduce O_2 [11]. The site for substrate oxidation includes one Cu ion known as the T1 site, whereas the O_2 reduction cluster comprises three Cu ions denoted as T2 and T3 sites [12]. BOx is able to accept electrons from electrodes biased with redox potentials lower than that of its Cu T1 site [11,12]. Furthermore, BOx is catalytically active at neutral pH and high chloride concentrations, unlike other MCOs, e.g. fungal laccases. Therefore, BOx is a suitable enzyme for creation of potentially implantable biosensors and biocathodes of biofuel cells. It shows some advantages over other oxidases like glucose oxidase, such as not producing H_2O_2, its suitability for direct electron transfer, a suitable potential range to avoid interferences, and a high activity at neutral pH.

* Corresponding authors. Tel.: +34 91 585 4813; fax: +34 91 585 4760.
E-mail addresses: marcospita@icp.csic.es (M. Pita), crisgs@icp.csic.es (C. Gutierrez-Sanchez), mdto@novozymes.com (M.D. Toscano), sergey.shleev@mah.se (S. Shleev), alopez@icp.csic.es (A.L. De Lacey).
[1] Tel.: +34 91 585 4813; fax: +34 91 585 4760.
[2] Tel.: +46 40 665 7414; fax: +46 40 665 8100.

1567-5394/$ – see front matter
http://dx.doi.org/10.1016/j.bioelechem.2013.07.001

BOx has already been a matter of bioelectronic development for biofuel cell applications [13–16]. Development of a BOx-based biosensor differs from biofuel cell cathodes: the former does not need a maximized current density while the latter does. Therefore the above-mentioned examples are not optimized for O_2 monitoring, especially for low O_2 concentrations.

Despite of the many publications concerning bioelectrochemical studies of MCO-modified electrodes in general, and BOx-based electrodes in particular, there are only few works reporting BOx-biomodified electrodes in physiological fluids [17,18]. Moreover, up to our best knowledge, mediator-less O_2-sensitive MCO-based sensors have not been designed so far.

The goal of the present work is to study the performance of BOx electrodes as O_2 biosensors, when immersed in a serum-mimicking buffer. BOx was covalently immobilized on Au nanoparticles (AuNPs)-modified Au electrodes [15], which where functionalized to optimize the direct electron transfer (DET) between the immobilized enzyme and the electrode surface. We have aimed obtaining a sensitive amperometric biosensor that may operate in buffer solutions and complex physiological fluids in the absence of membranes, which are known to be a kinetic barrier for electron transfer and mass transfer that lowers the classic biosensors performance. In order to minimize the energy requirements from a hypothetical implantable biofuel cell, the aimed biosensor is designed to work under global currents lower than 1 μA while being able to measure a wide range of O_2 concentrations.

2. Materials and methods

2.1. Enzyme

A highly purified preparation of *Myrothecium verrucaria* BOx (*Mv*BOx), expressed recombinantly in *Aspergillus oryzae*, has been kindly provided by Novozymes A/S (Denmark).

2.2. Chemicals

All reagents purchased were of ACS purity grade. 6-amino-2-naphtoic acid (NA), $NaNO_2$, 3-mercaptopropionic acid (MPA), $HAuCl_4$, sodium citrate, 1-(3-dimethylaminopropyl)-3-ethylcarbodiimide (EDC), N-hydroxysuccinimide (NHS), 30% H_2O_2, 2-morpholinoethanesulfonate (MES) hydrate 99.5% were purchased from Sigma-Aldrich (USA). 98% H_2SO_4, $NaH_2PO_4 \cdot 2H_2O$, $Na_2HPO_4 \cdot 12H_2O$ were purchased from Panreac (Spain). Water Milli-Q (18.2 MΩ cm) was used for all the experiments.

2.3. Gold nanoparticle synthesis

AuNPs were prepared following the method of $HAuCl_4$ reduction by citrate [19]. 125 mL of a 38.8 mM citrate solution was heated until boiling, and afterwards 12.5 mL of 1 mM $HAuCl_4$ solution was added. The reaction was allowed to proceed for 15 min and then cooled down to room temperature.

2.4. Modification of gold electrodes with AuNPs and BOx

Gold-disk electrodes (Metrohm, 2 mm diameter, 99.999% purity) were cleaned as previously reported [20]. The method for modifying Au electrodes with AuNPs is based on a previous report [15]. AuNPs were concentrated 100-fold by centrifugation. A single 15 μL drop of the concentrated AuNP dispersion was deposited on the surface of the electrodes and let to dry. Afterwards, the modified electrode was taken into an electrochemical cell containing 0.1 M H_2SO_4 and, in order to oxidize and reduce the gold surface, 20 cyclic voltammograms (CVs) were run from 0 to +1.5 V at 100 mV/s scan rate. The AuNP-Au electrode was immersed in an electrochemical cell filled with an ice-cooled solution, prepared immediately before its use by mixing 2 mL of 20 mM NA in acetronitrile and 2 mL of 2 mM $NaNO_2$ in 2 M HCl solution. A reductive CV from +0.6 V to −0.6 V at 200 mV/s was recorded. Later, the electrodes were immersed into a 1 mM MPA aqueous solution overnight. Finally, the electrodes were rinsed with water, dried with a gentle N_2 flow and immersed for 1 h in a 20 μL solution containing 0.83 mg/mL BOx in 10 mM MES buffer pH 6. Afterwards, the electrode was taken into a MES buffer solution containing 16 mM EDC and 32 mM NHS freshly prepared for 2 h. The electrode was then rinsed with 100 mM phosphate buffer, pH 7.4.

2.5. Buffers

Two buffers were used for the electrochemical studies, *viz.* 100 mM phosphate buffer, pH 7.4 (PBS) and a complex serum-like buffer (SLB), pH 7.4. The human SLB was prepared by the addition of 150 mM NaCl, 18 mM $NaHCO_3$, 5.55 mM glucose, 4.3 mM urea, 0.4 mM fructose, 0.4 mM uric acid, 0.055 mM ascorbic acid, 0.1 mM L-cysteine and 0.87 mM $MgSO_4$ into 100 mM PBS. This solution mimics quite well both the content and composition of human serum besides its protein content [21].

2.6. Electrochemical measurements

Experiments were performed with an Autolab PGSTAT30 analyzer controlled by GPES 4.9 software, Eco Chemie. The experiments were run in a three-electrode glass cell using a BAS Ag/AgCl/3 M KCl reference electrode (204 mV vs. NHE) and a platinum wire counter electrode. All redox potentials mentioned in the text and figures are given vs. Ag/AgCl/3 M KCl reference electrode. CVs were recorded from 0.7 to 0 V using a scan rate of 10 mV/s. Chronoamperometry was recorded at a constant potential of 0.1 V for 10,000 s.

2.7. UV-Vis spectroscopy

The measurements were performed with an UV-2401PC spectrophotometer (Shimadzu) under thermostatic conditions using disposable polycarbonate cuvettes.

2.8. Transmission electron microscopy (TEM)

200 KV JEOL 2100 transmission electron microscope equipped with an Oxford Instruments EDX analyzer was used for the analyses. Free software ImageJ 1.46R from NIH was used for nanoparticle statistic purposes. The sample was prepared by adding a drop of diluted AuNPs dispersion on a carbon-coated copper grid 200 Mesh and then let to dry.

3. Results and discussion

3.1. Nanoparticle characterization

AuNPs were synthesized as described above, and they were characterized by TEM and UV-Vis (Fig. 1). Analysis of the TEM images with ImageJ gave an AuNPs average size of 10.9 ± 2.3 nm by counting 240 nanoparticles (Fig. 1C). Besides, the AuNPs average size and concentration were determined from their localized surface plasmon resonance measured by UV-Vis spectroscopy [22]. The UV-Vis spectrum of a 10-fold diluted AuNPs dispersion showed a resonance-absorption band centered at $\lambda_{SPR} = 519$ nm with an absorbance of $A_{SPR} = 0.220$ (Fig. 1D). Another relevant parameter for the AuNPs characterization was $A_{450} = 0.141$. According to Haiss' numerical method [22], the synthesized nanoparticles were *ca.* 11 nm in diameter and dispersed at a concentration of approximately 17 nM. Therefore, the AuNPs size values determined by TEM and UV-Vis are coherent.

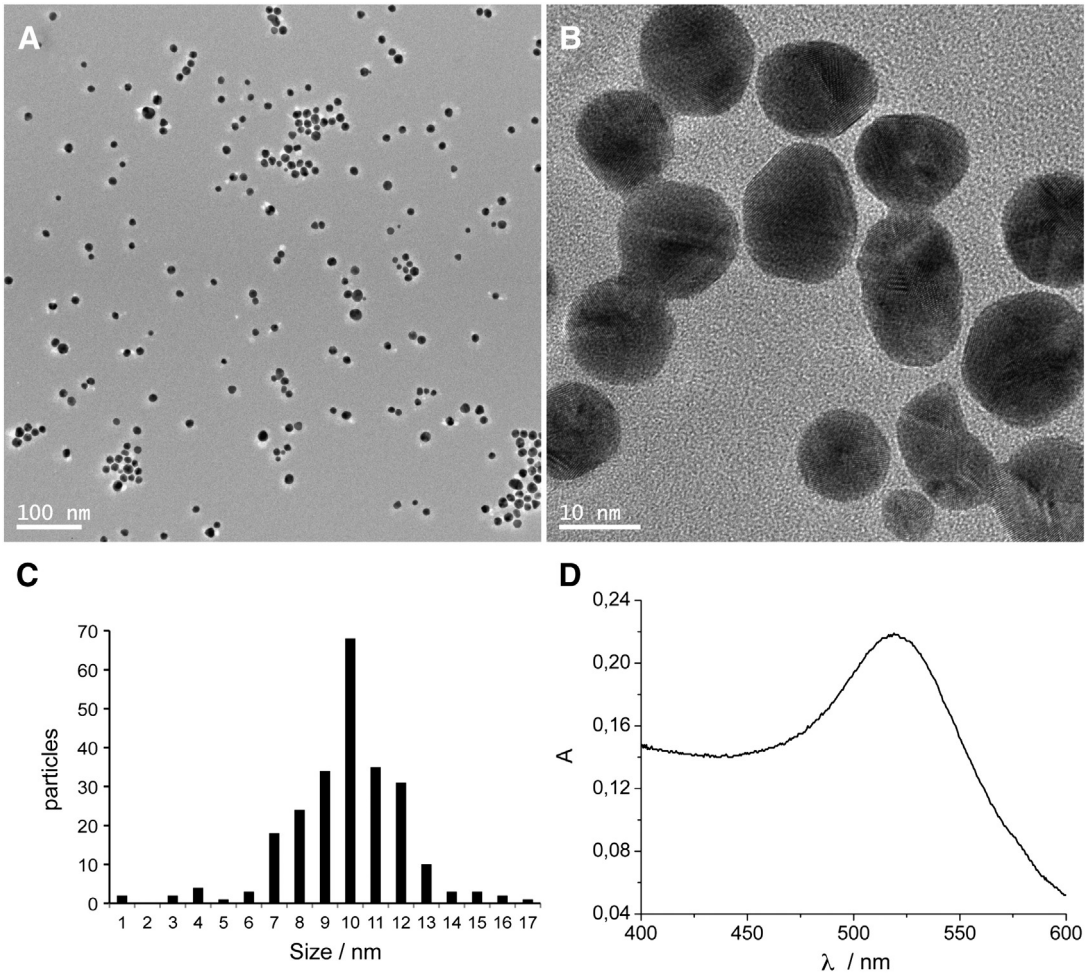

Fig. 1. AuNPs characterization. (A) Low magnification TEM picture. (B) High amplification TEM picture. (C) Particle size counts in Fig. 1A. (D) UV-Vis spectra of AuNPs dispersion 10-fold diluted.

3.2. Electrode modification

A clean Au-disk electrode was modified with the AuNPs dispersion to increase the surface area of the electrodes while maintaining their geometric area, and to favor DET with the immobilized enzyme. By consecutive AuNPs deposition cycles it is possible to linearly increase the electrode area [14], which is of interest for developing a highly sensitive O_2 biosensor based on BOx activity. The surface enhancement of the Au electrode after one deposition of AuNPs was estimated by integrating the Au reduction electrochemical wave (Fig. S1). As a side effect, the capacitive current of the modified gold electrode was slightly increased in the region where the biosensor's measuring potential will be applied (Fig. S1, inset). The non-modified gold electrode had an electroactive surface of 0.068 cm^2, whereas the deposition of AuNPs allowed an increase of *ca.* 30-fold, reaching about 2 cm^2 area. The successive cycling of the electrode surface causes a decrease of the gold reduction area, which is attributed to the alloying of the particles with each other and therefore the final electroactive area can be controlled (Fig. S2). The enhancement was considered sufficient for developing a sensitive biosensor, allowing for a higher bioelectrocalytic signal.

The AuNPs modified electrode was modified with a mixed monolayer designed to favor the DET of BOx. Modification of a graphite electrode with 6-naphtocarboxylic groups has been proven to facilitate DET of BOx at graphite electrodes [23]. By a similar procedure, we have made 6-amino-2-naphtoic acid inside the electrochemical cell react with $NaNO_2$ and HCl to synthesize the diazonium salt derivative. A fast CV was run to reduce the diazonium salt and to form a NA layer *via* Au-C bonds [20,24]. This modification method hampers the formation of multiple layers but unfortunately yields an incomplete coverage of the surface, therefore an additional thiol self-assembled monolayer (SAM) is needed to protect the enzyme molecules from denaturizing by direct gold contact [20]. MPA has proven to support DET process between gold and BOx [25–27], so it was chosen to build a thiol SAM on the Au surface by immersion of the NA-AuNPs electrode in a 1 mM MPA solution overnight. AuNPs have also played a role in facilitating other DET processes between an electroactive surface of low-density graphite and a different MCO, *Trametes hirsuta* laccase [28]. In that case a high potential Nernstian-dependent electrocatalytic process was observed by cyclic voltammetry, which was attributed to the wiring of laccase via the AuNP. However, in the present work that effect does not appear and AuNPs do not seem to play such electronic role in the DET process.

The MPA/NA-AuNPs Au electrode was used for the covalent immobilization of BOx *via* formation of amide bonds between the carboxylic groups at the Au surface and the lysine residues of the enzyme. The nanostructured electrodes modified with BOx were firstly tested by cyclic voltammetry in 100 mM PBS (Fig. 2A). It should be noted that the immobilized BOx required electrochemical activation before offering an appropriate electrocatalytic signal, thus a CV between 0.7 and 0 V was performed prior to the analysis. Similar electrocatalytic behavior has already been reported very recently for BOx adsorbed on graphite electrodes and has been attributed to the reductive activation at low potential of the enzyme in the "alternative resting" form [29]. Afterwards, the two CVs shown in Fig. 2A were recorded. The first one was measured in O_2-saturated solution and the second

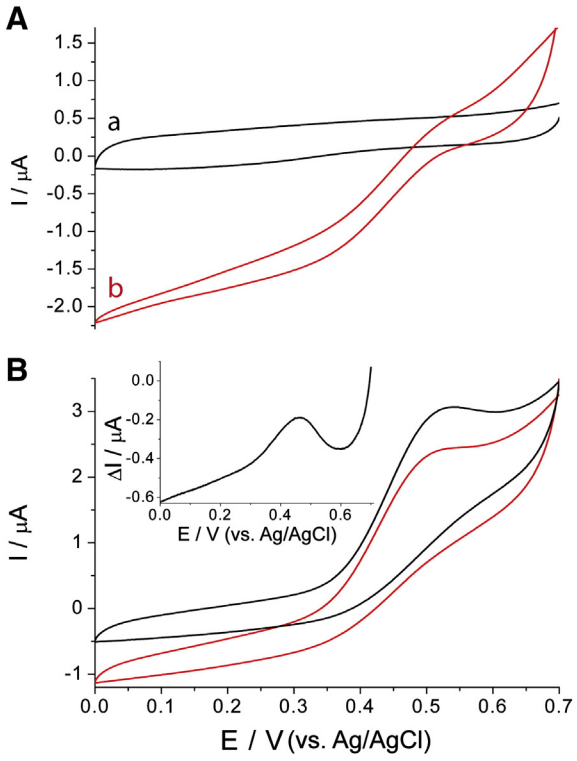

Fig. 2. Cyclic voltammograms of *Mv*BOx-MPA/NA-AuNPs electrode (A) in PBS; (B) in SLB. (a) N_2-saturated, (b) O_2 saturated. Inset in (B) corresponds to the subtraction of the CVs' forward scans.

one in N_2-saturated solution. A clear bioelectrocatalytic process for O_2 reduction is observed starting at 0.52 V, which is near to the redox potential of the T1 site of *Mv*BOx [30]. There is a fast increase of the current value until 0.35 V, where the current increase slows down but does not reach the theoretical plateau for an electrocatalytic process. The residual slope of the bioelectrocatalytic current at high overpotentials is typical for BOx-based biocathodes, when O_2 transport is not rate-limiting the bioelectrocatalytic process. It indicates that a dispersion of interfacial electron transfer rates is affecting the bioelectrocatalysis, even if a preferential orientation of the immobilized BOx is favored [23]. This limitation of the measured current by the enzyme DET may affect the stability and reproducibility of the biosensor. This DET-based rate limitation could be diminished increasing the amount of immobilized BOx on the electrode surface. However, in that case the overall measured current would be greatly increased, which is an undesired effect for our goals. The catalytic current obtained after saturating the cell atmosphere and solution with N_2 is almost negligible, as expected for a system with a very low O_2 concentration. It has been reported that in human serum the electrochemical response of BOx can be diminished [31], so after testing that the electrode was active, it was taken into a cell filled with the SLB to evaluate its electrochemical response (Fig. 2B). It should be noted that serum proteins have not been considered because they can be easily avoided using big pore size membranes and have no inhibitory effect on BOx; all other small compounds considered cannot be easily blocked and may hamper the bioelectrocatalytic performance.

At first sight the CVs obtained show several differences with the ones recorded in PBS. The presence of redox active interferences such as uric and ascorbic acids causes a high oxidative current above 0.35 V that diminishes the biocatalytic reductive current measured at the higher potentials due to BOx activity. In other words, depolarization of biocathodes in human physiological fluids occurs [18]. The resulting CVs also show that the O_2 reduction current measured in SLB for values lower than 0.35 V is reduced approximately 50% vs. the current measured for PBS. The decrease in the current at low oxidative potentials can be attributed to several factors, such as the high concentration of chloride and other compounds in the medium, which may cause a reversible and partial inhibition of BOx [19,32], or the lower solubility of O_2 in the serum buffer than in PBS [6].

The need of our step-by-step modified nanostructured electrode was justified with a control experiment in the absence of AuNPs (Fig. 3), where much lower currents were measured from the BOx bioelectrocatalytic signal. The surface area enhancement caused by the AuNPs deposition appears as a critical strategy to develop the biosensing performance by tuning the electroactive area available for hosting the biocatalyst, and thus the catalytic current measured.

Another control experiment was done in which the AuNPs-Au electrode was modified only with MPA and BOx. The results showed that, despite offering a comparable bioelectrocatalytic signal in PBS, the system did not work in the SLB (Fig. 4). This behaviour may be related to the lower stability of thiols SAM on gold compared to monolayers prepared by diazonium salts reduction [33].

3.3. Biosensor performance

The performance of the O_2 biosensor in SLB was studied by chronoamperometry at 0.1 V to minimize the interference of uric and ascorbic acids (Fig. 3). Aliquots of an O_2 saturated SLB ($[O_2]_{sat}$ = 1.27 mM) were gradually added to the electrochemical cell, filled with N2 saturated SLB, recording the maximum value of reductive transient current measured after each addition. This method allows a fast time-response and a reliable calibration at low O_2 concentrations. At the end of the experiment the solution was bubbled again with N_2 and the background current was reached again (Figure S3, Table S1). The concentration of O_2 was correlated with the peak current values reached in the injections, obtaining a linear relationship for values below 300 mM (Fig. 5), which is approximately the concentration of O_2 in an air-equilibrated solution. The fitted linear equation for this range, which shows an r factor of -0.997, is the following:

$$I(\mu A) = -0.054 - (0.9 \pm 0.1)\ [O_2]\ (mM) \quad (1)$$

The reproducibility of 3 replicate calibrationswaswithin a 17% relative standard deviation and the O2 detection limit was 6 ± 1 μM. The sensitivity obtained was −0.9 ± 0.1 μA/mM.

4. Conclusions

The bioelectronic system developed by modifying an Au electrode with AuNPs and further functionalized for the covalent attachment of BOx was able to function as O_2 biosensor in a solution mimicking the composition and content of human serum. A linear response was measured in the broad range of 6–300 μM. Thus, the detection range of the

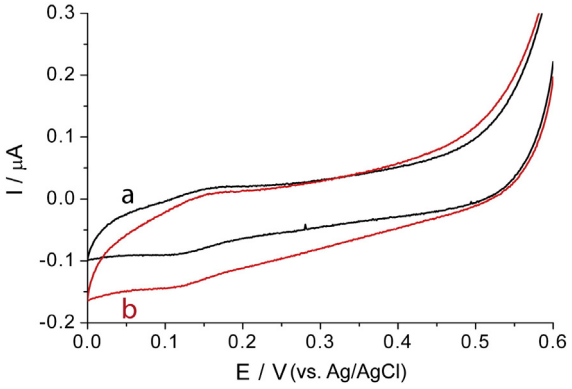

Fig. 3. CVs of a gold disc electrode modified with a mixed monolayer of 6-carboxynaphtoyl and MPA groups and BOx in PBS. (a) Saturated with N_2, (b) saturated with O_2.

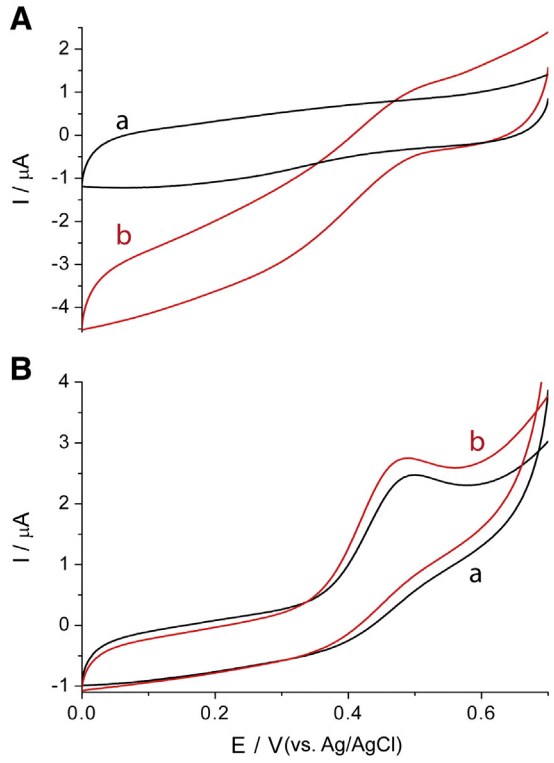

Fig. 4. CVs of a BOx-MPA-AuNP-Au electrode. (A) PBS electrolyte (a) saturated with N_2, (b) saturated with O_2. (B) SLB electrolyte (a) saturated with N_2, (b) Saturated with O_2.

design biosensor is very suitable for both *ex vivo* (air saturated biological fluids, where oxygen concentration will be close to 0.25 mM) and *in vivo* (natural biological fluids, where oxygen concentration will be in mM range) studies. The presented biosensor will be used together with implantable biofuel cells [18,34,35], aiming at producing implantable nanobiodevices able to work *in vivo* using biological fluids as fuel and emitting the signals registered to an external transducing device. Future work will focus on the study of a BOx-based biosensor in other biofluids with different pH and saline conditions, analyzing the potential differences caused by the new environmental conditions.

Supplementary data to this article can be found online at http://dx.doi.org/10.1016/j.bioelechem.2013.07.001.

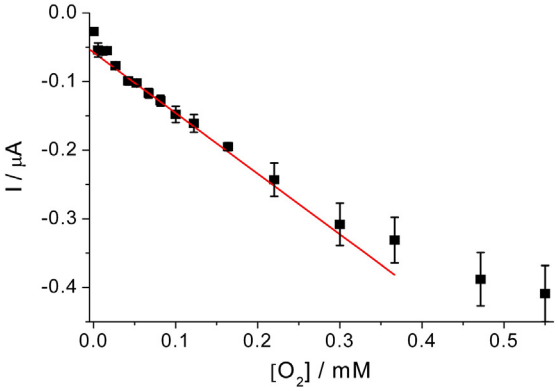

Fig. 5. Calibration curve of a BOx-MPA/NA-AuNPs-Au electrode in SLB measured at 0.1 V vs. Ag/AgCl. The calibration in Eq. (1) is shown in the text.

Acknowledgments

This work was funded by the FP7 project "3D-Nanobiodevice" (NMP4-SL-2009-229255). We thank Novozymes A/S for the preparation of *Myrothecium verrucaria* BOx. M.P. acknowledges the 2009 Ramon y Cajal program from the Spanish MINECO.

References

[1] A.K. Shukla, P. Suresh, S. Berchmans, A. Rajendran, Biological fuel cells and their applications, Curr. Sci. 87 (2004) 455–468.
[2] F. Davis, S.P.J. Higson, Biofuel cells—recent advances and applications, Biosens. Bioelectron. 22 (2007) 1224–1235.
[3] A.C. Guyton, J.E. Hall, Textbook of Medical Physiology, 11th ed. Saunders-Elsevier, Philadelphia, 2006.
[4] I. Silver, M. Erecinska, Extracellular glucose concentration in mammalian brain: continuous monitoring of changes during increased neuronal activity and upon limitation in oxygen supply in normo-, hypo-, and hyperglycemic animals, J. Neurosci. 14 (1994) 5068–5076.
[5] F. Cohen, G. Burdairon, F. Rouelle, M. Chemla, Electrochemical analysis of oxygen content in samples of whole human saliva, Electroanalysis 1 (1989) 523–527.
[6] M.L. Hitchman, Measurement of Dissolved Oxygen, John Wiley & Sons, New York, 1978.
[7] G. Jobst, G. Urban, A. Jachimowicz, F. Kohl, O. Tilado, I. Lettenbichler, G. Nauer, Thin-film Clark-type oxygen sensor based on novel polymer membrane systems for in vivo and biosensor applications, Biosens. Bioelectron. 8 (1993) 123–128.
[8] C. Chan, M. Lehmann, K. Chan, P. Chan, C. Chan, B. Gruendig, G. Kunze, R. Renneberg, Designing an amperometric thick-film microbial BOD sensor, Biosens. Bioelectron. 15 (2000) 343–353.
[9] C. Gutiérrez-Sánchez, M. Pita, M.D. Toscano, A.L. De Lacey, Bilirubin oxidase-based nanobiocathode working in serum-mimic buffer for implantable biofuel cell, Electroanalysis 25 (2013) 1359–1362.
[10] E. Solomon, U.M. Sundaram, T.E. Machonkin, Multicopper oxidases and oxygenases, Chem. Rev. 96 (1996) 2563–2605.
[11] N. Mano, Features and applications of bilirubin oxidases, Appl. Microbiol. Biotechnol. 96 (2012) 301–307.
[12] S. Shleev, J. Tkac, A. Christenson, T. Ruzgas, A.I. Yaropolov, J.W. Whittaker, L. Gorton, Direct electron transfer between copper-containing proteins and electrodes, Biosens. Bioelectron. 20 (2005) 2517–2554.
[13] S. Shleev, A. Kasmi, T. Ruzgas, L. Gorton, Direct heterogeneous electron transfer reactions of bilirubin oxidase at a spectrographic graphite electrode, Electrochem. Commun. 6 (2004) 934–939.
[14] S. Tsujimura, Y. Kamitaka, K. Kano, Diffusion-controlled oxygen reduction on multi-copper oxidase-adsorbed carbon aerogel electrodes without mediator, Fuel Cells 7 (2007) 463–469.
[15] K. Murata, K. Kajiya, N. Nakamura, H. Ohno, Direct electrochemistry of bilirubin oxidase on three-dimensional gold nanoparticle electrodes and its application in a biofuel cell, Energy Environ. Sci. 2 (2009) 1280–1285.
[16] U. Salaj-Kosla, S. Pöller, Y. Beyl, M.D. Scanlon, S. Beloshapkin, S. Shleev, W. Schuhmann, E. Magner, Direct electron transfer of bilirubin oxidase (*Myrothecium verrucaria*) at an unmodified nanoporous gold biocathode, Electrochem. Commun. 16 (2012) 92–95.
[17] C. Kang, H. Shin, A. Heller, On the stability of the "wired" bilirubin oxidase oxygen cathode in serum, Bioelectrochemistry 68 (2006) 22–26.
[18] M. Falk, V. Andoralov, Z. Blum, J. Sotres, D. Suyatin, T. Ruzgas, T. Arnebrant, S. Shleev, Biofuel cell as a power source for electronic contact lenses, Biosens. Bioelectron. 37 (2012) 38–45.
[19] G. Frens, Controlled nucleation for the regulation of the particle size in monodisperse gold suspensions, Nat. Phys. Sci. 241 (1973) 20–22.
[20] M. Pita, C. Gutierrez-Sanchez, D. Olea, M. Velez, C. Garcia-Diego, S. Shleev, V.M. Fernandez, A.L. De Lacey, High redox potential cathode based on laccase covalently attached to gold electrode, J. Phys. Chem. C 115 (2011) 13420–13428.
[21] K. Jung, Tietz Fundamentals of Clinical Chemistry, in: C.A. Burtis, E.R. Ashwood, D.E. Bruns (Eds.), 6th ed., Saunders/Elsevier, St. Louis, 2008.
[22] W. Haiss, N.T.K. Thanh, J. Aveyard, D.B. Fernig, Determination of size and concentration of gold nanoparticles from uv-vis spectra, Anal. Chem. 79 (2007) 4215–4221.
[23] L.D. dos Santos, V. Climent, C.F. Blanford, F.A. Armstrong, Mechanistic studies of the 'blue' Cu enzyme, bilirubin oxidase, as a highly efficient electrocatalyst for the oxygen reduction reaction, Phys. Chem. Chem. Phys. 12 (2010) 13962–13974.
[24] L. Laurentius, S.R. Stoyanov, S. Gusarov, A. Kovalenko, R. Du, G.P. Lopinski, M.T. McDermott, Diazonium-derived aryl films on gold nanoparticles: evidence for a carbon–gold covalent bond, ACS Nano 5 (2011) 4219–4227.
[25] P. Ramirez, N. Mano, R. Andreu, T. Ruzgas, A. Heller, L. Gorton, S. Shleev, Direct electron transfer from graphite and functionalized gold electrodes to T1 and T2/T3 copper centers of bilirubin oxidase, Biochim. Biophys. Acta Bioenerg. 1777 (2008) 1364–1369.
[26] M. Tominaga, M. Ohtani, I. Taniguchi, Gold single-crystal electrode surface modified with self-assembled monolayers for electron tunnelling with bilirubin oxidase, Phys. Chem. Chem. Phys. 10 (2008) 6928–6934.
[27] V. Climent, J. Zhang, E.P. Friis, L.H. Ostergaard, J.J. Ulstrup, Voltammetry and single-molecule in situ scanning tunnelling microscopy of laccases and bilirubin

oxidase in electrocatalytic dioxygen reduction on Au(111) single-crystal electrodes, Phys. Chem. C 116 (2012) 1232–1243.
[28] C. Gutierrez-Sanchez, M. Pita, C. Vaz-Domínguez, S. Shleev, A.L. De Lacey, Gold nanoparticles as electronic bridges for laccase-based biocathodes, J. Am. Chem. Soc. 134 (2012) 17212–17220.
[29] C.H. Kjaergaard, F. Durand, F. Tasca, M.F. Qayyum, B. Kauffmann, S. Gounel, E. Suranitu, K.O. Hodgson, B. Hedmann, N. Mano, E.I. Solomon, Spectroscopic and crystallographic characterization of "alternative resting" and "resting oxidized" enzyme forms of bilirubin oxidase: implications for activity and electrochemical behavior of multicopper oxidases, J. Am. Chem. Soc. 134 (2012) 5548–5551.
[30] A. Christenson, S. Shleev, N. Mano, A. Heller, L. Gorton, Redox potentials of the blue copper sites of bilirubin oxidases, Biochim. Biophys. Acta 1757 (2006) 1634–1641.
[31] V. Coman, R. Ludwig, W. Harreither, D. Haltrich, L. Gorton, T. Ruzgas, S. Shleev, A direct electron transfer-based glucose/oxygen biofuel cell operating in human serum, Fuel Cells 10 (2010) 9–16.
[32] S. Murao, N. Tanaka, Isolation and identification of a microorganism producing bilirubin oxidase, Agric. Biol. Chem. 46 (1982) 2031–2034.
[33] G. Liu, T. Böcking, J.J. Gooding, Diazonium salts: stable monolayers on gold electrodes for sensing applications, J. Electroanal. Chem. 600 (2007) 335–344.
[34] X.J. Wang, M. Falk, R. Ortiz, H. Matsumura, J. Bobacka, R. Ludwig, M. Bergelin, L. Gorton, S. Shleev, Mediatorless sugar/oxygen enzymatic fuel cells based on gold nanoparticle-modified electrodes, Biosens. Bioelectron. 31 (2012) 219–225.
[35] M. Falk, Z. Blum, S. Shleev, Direct electron transfer based enzymatic fuel cells, Electrochim. Acta 82 (2012) 191–202.